

NMR Study of Intramolecular and Intermolecular Ligand Exchange in Phenyltrifluorophosphorane¹

RONALD KIRK MARAT and ALEXANDER F. JANZEN*

Received June 11, 1979

Intramolecular axial-equatorial exchange and base-initiated intermolecular fluorine exchange in phenyltrifluorophosphorane have been studied by the dynamic NMR technique. Axial-equatorial exchange appears to be a unimolecular process with $\Delta G^*_{298} = 13.3 \pm 0.5$ kcal/mol, $\Delta H^* = 12.6 \pm 0.4$ kcal/mol, $\Delta S^* = -2.1 \pm 1.3$ eu, and $E_a = 13.2 \pm 0.4$ kcal/mol. Addition of triethylamine or pyridine to $C_6H_5PF_3H$ leads to intermolecular fluorine exchange. Rate studies of the intermolecular process support a mechanism involving slow production of $C_6H_5PF_4H^-$ followed by rapid fluorine transfer between five- and six-coordinate species $C_6H_5PF_3H$ and $C_6H_5PF_4H^-$. Although traces of HF and H_2O impurities did not interfere with this study, the impurity $C_6H_5PF_4$ markedly affected the NMR results. The intramolecular process is not correlated with the intermolecular process, and phosphorus-hydrogen coupling is retained throughout the rapid intermolecular fluorine-exchange process.

Introduction

Earlier studies in our laboratory have demonstrated that intermolecular fluorine, proton, and silyl exchange can be slowed down by removing HF,^{2,3} HCl,⁴ or H_2O ⁵ impurities. In the absence of these impurities fluorine transfer among silicon compounds occurs via fluorine-bridged species.⁶ The role of a Lewis base catalyst in the exchange process has also been investigated.^{2,6} As a continuation of this work, we have carried out a dynamic NMR study of intramolecular axial-equatorial exchange and base-initiated intermolecular fluorine exchange in phenyltrifluorophosphorane.

Experimental Section

Reagents. Benzene, deuteriobenzene, and toluene were stored over generous quantities of 4A molecular sieve. Nitromethane was washed with an equal volume of saturated aqueous sodium carbonate and then twice with equal volumes of water, dried with $MgSO_4$, distilled from 4A molecular sieve, and stored over 4A molecular sieve. Acetonitrile was distilled from P_2O_5 and stored over 3A molecular sieve. Triethylamine was distilled from NaOH pellets and stored over 4A molecular sieve; pyridine, quinoline, 2,6-lutidine, and 4-picoline were stored over 4A molecular sieve.

$C_6H_5PF_2$ was prepared by the method of Schmutzler.⁷ It is known to decompose upon standing to give $C_6H_5PF_4$ and $(C_6H_5P)_5$. This decomposition could be slowed down by storing $C_6H_5PF_2$ in a Teflon bottle at $-20^\circ C$. After the solution stood for some time, $C_6H_5PF_2$ was purified by adding a small amount of quinoline (to form the quinoline adduct of $C_6H_5PF_4$) and distilling out $C_6H_5PF_2$ at reduced pressure.

$C_6H_5PF_3H$ was prepared by careful addition of a solution of HF in acetonitrile (~ 5 M) to a sample of freshly prepared $C_6H_5PF_2$ (10 g) at $0^\circ C$. The addition was monitored by ^{19}F NMR. The product was then distilled through a 15-cm Vigreux column to give $C_6H_5PF_3H$ (8.9 g, 78% yield), bp $58-63^\circ C$ at 25 torr. $C_6H_5PF_3H$ was stored in a Teflon bottle at $-20^\circ C$ and handled in a nitrogen filled drybox. Samples of $C_6H_5PF_3H$ prepared in this manner were contaminated by 0.2-3 mol % $C_6H_5PF_4$.

NMR Spectra. The NMR spectra were obtained on a Bruker WH-90 spectrometer at 36.44 MHz (^{31}P), 90 MHz (1H), and 84.66

MHz (^{19}F). Proton and fluorine NMR spectra were also obtained on a Varian A-56/60A spectrometer at 60 MHz (1H) and 56.4 MHz (^{19}F). All line shape calculations were performed on an IBM 370-168 computer using the Fortran H (extended) compiler and a modified version of the program EXCHSYS.^{3,8,9}

NMR sample tubes were thoroughly cleaned, treated with hexamethyldisilazane, and heated to $200^\circ C$ for at least 12 h. NMR samples were prepared in a nitrogen filled drybox with the aid of various micro syringes and an automatic pipet. The samples were allowed to equilibrate in the NMR spectrometer for about 5 min and then recorded as rapidly as possible. Consistent NMR results were only obtained after careful purification of reagents and solvents.

Results and Discussion

Line Shape Calculations. The proton-decoupled ^{31}P and 1H NMR line shapes for $C_6H_5PF_3H$ may be calculated by standard probability matrix techniques¹⁰ since all lines are independent except for the effects of chemical exchange. The $^{31}P\{^1H\}$ NMR spectrum of "rigid" trigonal-bipyramidal $C_6H_5PF_3H$ consists of six lines corresponding to the six possible fluorine spin states. Two matrices describe the transfer of magnetization between lines for either intramolecular (P_{intra})

$$P_{intra} = \begin{matrix} & \begin{matrix} 1 & 2 & 3 & 4 & 5 & 6 \end{matrix} & & \begin{matrix} F_{eq} \\ F_{ax} \end{matrix} \\ \begin{matrix} 1 \\ 2 \\ 3 \\ 4 \\ 5 \\ 6 \end{matrix} & \begin{bmatrix} 0 & 0 & 0 & 0 & 0 & 0 \\ 0 & -1/2 & 0 & 1/2 & 0 & 0 \\ 0 & 0 & -1 & 0 & 1 & 0 \\ 0 & 1 & 0 & 1 & 0 & 0 \\ 0 & 0 & 1/2 & 0 & -1/2 & 0 \\ 0 & 0 & 0 & 0 & 0 & 0 \end{bmatrix} & \begin{matrix} \alpha & \alpha\alpha \\ \alpha & 1/\sqrt{2}(\alpha\beta + \beta\alpha) \\ \alpha & \beta\beta \\ \beta & \alpha\alpha \\ \beta & 1/\sqrt{2}(\alpha\beta + \beta\alpha) \\ \beta & \beta\beta \end{matrix} \end{matrix}$$

or intermolecular (P_{inter}) exchange of fluorine ligands. Each

$$P_{inter} = \begin{matrix} & \begin{matrix} 1 & 2 & 3 & 4 & 5 & 6 \end{matrix} & & \begin{matrix} F_{eq} \\ F_{ax} \end{matrix} \\ \begin{matrix} 1 \\ 2 \\ 3 \\ 4 \\ 5 \\ 6 \end{matrix} & \begin{bmatrix} -1/2 & 1/3 & 0 & 1/6 & 0 & 0 \\ 1/6 & -1/2 & 1/6 & 0 & 1/6 & 0 \\ 0 & 1/3 & -1/2 & 0 & 0 & 1/6 \\ 1/6 & 0 & 0 & -1/2 & 1/3 & 0 \\ 0 & 1/6 & 0 & 1/6 & -1/2 & 1/6 \\ 0 & 0 & 1/6 & 0 & 1/3 & -1/2 \end{bmatrix} & \begin{matrix} \alpha & \alpha\alpha \\ \alpha & 1/\sqrt{2}(\alpha\beta + \beta\alpha) \\ \alpha & \beta\beta \\ \beta & \alpha\alpha \\ \beta & 1/\sqrt{2}(\alpha\beta + \beta\alpha) \\ \beta & \beta\beta \end{matrix} \end{matrix}$$

matrix element p_{ij} is the probability that a phosphorus atom having a resonance frequency defined by state i will have a

(1) Presented at the Fourth Winter Fluorine Conference, Daytona Beach, FL, Jan 28-Feb 2, 1979.
(2) A. F. Janzen, J. A. Gibson, and D. G. Ibbott, *Inorg. Chem.*, **11**, 2853 (1972); D. G. Ibbott and A. F. Janzen, *Can. J. Chem.*, **50**, 2428 (1972); J. A. Gibson, D. G. Ibbott, and A. F. Janzen, *ibid.*, **51**, 3203 (1973).
(3) R. K. Marat and A. F. Janzen, *Can. J. Chem.*, **55**, 1167 (1977).
(4) A. Queen, A. E. Lemire, A. F. Janzen, and M. N. Paddon-Row, *Can. J. Chem.*, **56**, 2884 (1978).
(5) R. E. Wasylshen, G. S. Birdi, and A. F. Janzen, *Inorg. Chem.*, **15**, 3054 (1976).
(6) R. K. Marat and A. F. Janzen, *Can. J. Chem.*, **55**, 3845 (1977).
(7) R. Schmutzler, *Chem. Ber.*, **98**, 552 (1965).

(8) J. K. Krieger, Ph.D. Thesis, Massachusetts Institute of Technology, Cambridge, MA, 1971.
(9) R. K. Marat, M.Sc. Thesis, University of Manitoba, Winnipeg, Manitoba, 1976.
(10) R. Kubo, *Nuovo Cimento, Suppl.*, **6**, 1063 (1957); R. A. Sack, *Mol. Phys.*, **1**, 163 (1958); C. S. Johnson, Jr., *J. Chem. Phys.*, **41**, 3277 (1964); L. W. Reeves and K. N. Shaw, *Can. J. Chem.*, **48**, 3641 (1970).

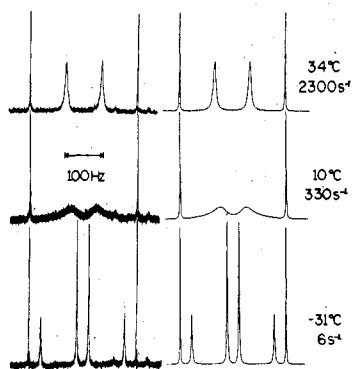


Figure 1. Typical temperature-dependent experimental (left) and calculated (right) $^{31}\text{P}\{^1\text{H}\}$ NMR spectra of $\text{C}_6\text{H}_5\text{PF}_3\text{H}$ showing intramolecular axial-equatorial fluorine exchange.

resonance frequency defined by state j after the exchange. The diagonal element p_{ii} is the probability that magnetization will leave line i during the exchange. A negative sign indicates transfer of magnetization out of the line.

For simultaneous intra- and intermolecular fluorine exchange, the two probability matrices may be combined into one matrix R (eq 1) describing the rate of transfer of magnetization between lines, where τ_{intra} and τ_{inter} are the preexchange lifetimes for intramolecular and intermolecular exchange.

$$R = P_{\text{intra}}\tau_{\text{intra}}^{-1} + P_{\text{inter}}\tau_{\text{inter}}^{-1} \quad (1)$$

The derivation of P_{inter} assumes equal exchange probabilities for the equatorial and each of the axial fluorines. Spectra calculated with half or twice this statistical probability, at constant $\tau_{\text{intra}}^{-1} = 900 \text{ s}^{-1}$ (characteristic of spectra recorded at 22°C), showed only minor changes in the line shape, resulting in a maximum error of 5–10% in the determination of τ_{inter}^{-1} .

Intra- and intermolecular exchange was observed by using either $^{31}\text{P}\{^1\text{H}\}$ or ^1H NMR. Each half of the P–H doublet in the ^1H NMR has the same number of lines, corresponding to the same fluorine spin states, as the $^{31}\text{P}\{^1\text{H}\}$ spectrum; therefore, the same probability matrices are used. P–H coupling was not included in the line shape calculations because multiplets do not overlap and the P–H bond is not broken during the exchange process.

Although it was possible to study intramolecular exchange in the absence of intermolecular exchange, since the latter only occurs after addition of base, it proved impossible to study intermolecular exchange in the absence of intramolecular exchange because of intramolecular line-broadening effects over the entire temperature range where intermolecular exchange could be studied. Consequently, τ_{intra} was first obtained over the accessible temperature range in the absence of base, by comparison of calculated and experimental spectra. After addition of base, the spectra were recorded and compared to spectra calculated with various values of τ_{inter} but with the value of τ_{intra} calculated above. Typical calculated and experimental $^{31}\text{P}\{^1\text{H}\}$ NMR spectra for the intra- and intermolecular processes are shown in Figures 1 and 2.

On the assumption that intramolecular exchange is independent of phosphorane concentration, the first-order rate constant is equal to the reciprocal preexchange lifetime (eq 2). For intermolecular exchange, the preexchange lifetime

$$\tau_{\text{intra}}^{-1} = k_{\text{intra}} \quad (2)$$

may be related to the rate constant by

$$\tau_{\text{inter}}^{-1} = \frac{1}{3}k_{\text{inter}}[\text{C}_6\text{H}_5\text{PF}_3\text{H}]^{a-1}[\text{base}]^b \quad (3)$$

where a is the kinetic order in phosphorane and b is the order

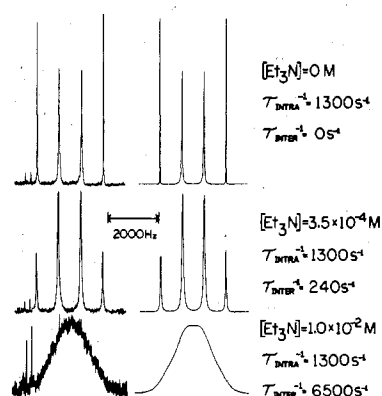


Figure 2. Typical experimental (left) and calculated (right) $^{31}\text{P}\{^1\text{H}\}$ NMR spectra of Et_3N -initiated intermolecular fluorine exchange in $\text{C}_6\text{H}_5\text{PF}_3\text{H}$ at 28°C at a constant rate of intramolecular exchange.

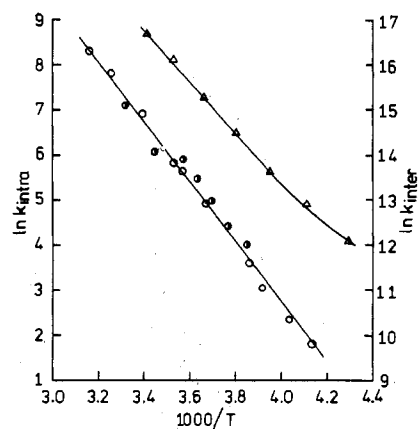


Figure 3. Plots of $\ln k_{\text{intra}}$ and $\ln k_{\text{inter}}$ vs. $1/T$: \circ , intramolecular exchange, ^1H NMR, $[\text{C}_6\text{H}_5\text{PF}_3\text{H}] = 1.96 \text{ M}$ in CH_2Cl_2 ; \bullet , intramolecular exchange, $^{31}\text{P}\{^1\text{H}\}$ NMR, $[\text{C}_6\text{H}_5\text{PF}_3\text{H}] = 3.3 \text{ M}$ in 2:1 v/v $\text{CH}_3\text{NO}_2/\text{C}_6\text{H}_6$; Δ , intermolecular exchange, $^{31}\text{P}\{^1\text{H}\}$ NMR, $[\text{C}_6\text{H}_5\text{PF}_3\text{H}] = 0.35 \text{ M}$, $[\text{C}_2\text{H}_5\text{N}] = 0.0076 \text{ M}$ in 2:1 v/v toluene/ C_6D_6 .

in base.^{3,11} The orders may be found experimentally by log-log plots of τ_{inter}^{-1} vs. $\text{C}_6\text{H}_5\text{PF}_3\text{H}$ and base concentration. Error limits in activation parameters were determined by a two-parameter fit.¹⁶ Systematic errors in ΔS^\ddagger may be larger because of the long extrapolation involved.

Intramolecular Axial-Equatorial Fluorine Exchange. The effect of temperature on axial-equatorial exchange is shown in Figure 3. A least-squares analysis of the data in Figure 3 gives the following activation parameters for axial-equatorial exchange: $\Delta G^\ddagger_{298} = 13.3 \pm 0.5 \text{ kcal/mol}$, $\Delta H^\ddagger = 12.6 \pm 0.4 \text{ kcal/mol}$, $\Delta S^\ddagger = -2.1 \pm 1.3 \text{ eu}$, and $E_a = 13.2 \pm 0.4 \text{ kcal/mol}$.

A number of experiments support the view that axial-equatorial exchange in $\text{C}_6\text{H}_5\text{PF}_3\text{H}$ is a unimolecular process. Thus the exchange rate was found to be independent of $\text{C}_6\text{H}_5\text{PF}_3\text{H}$ concentration over at least a 10-fold concentration range, from 0.15 to 1.5 M. The rate was also found to be independent of solvent, as seen in Figure 3 where the points for a nitromethane solution lie along the same line as for a methylene chloride solution. Even a basic solvent such as tetrahydrofuran, which causes a rate increase in RPF_4 compounds,¹² had no measurable effect on the NMR spectrum. Presumably, coordination with tetrahydrofuran does not

- (11) A. A. Frost and R. G. Pearson, "Kinetics and Mechanism", 2nd ed., Wiley, New York, 1961; L. W. Reeves, *Adv. Phys. Org. Chem.*, **3**, 187 (1965); G. Binsch, "Dynamic Nuclear Magnetic Resonance Spectroscopy", L. M. Jackman and F. A. Cotton, Eds., Academic Press, New York, 1975.
- (12) M. Eisenhut, H. L. Mitchell, D. D. Traficante, R. J. Kaufman, J. M. Deutch, and G. M. Whitesides, *J. Am. Chem. Soc.*, **96**, 5385 (1974).

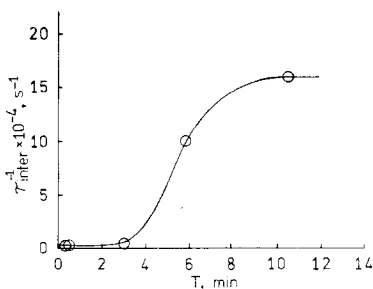


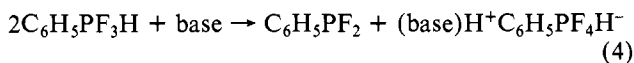
Figure 4. Plot of τ_{inter}^{-1} vs. time at 22 °C. $[\text{C}_6\text{H}_5\text{PF}_3\text{H}] = 0.5 \text{ M}$ and $[\text{C}_5\text{H}_5\text{N}] = 0.0175 \text{ M}$.

equilibrate axial and equatorial fluorines, or, alternatively, $\text{C}_6\text{H}_5\text{PF}_3\text{H}$ is a weaker Lewis acid than RPF_4 . The small activation entropy is also in agreement with a unimolecular process.

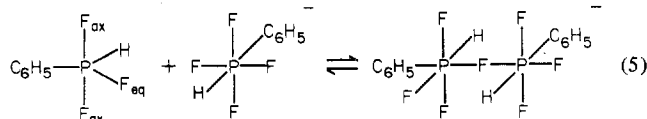
It is possible to measure, simultaneously, the intramolecular- and intermolecular-exchange rate in the presence of base under conditions of moderate intramolecular and slow intermolecular exchange. Since the intramolecular-exchange rate under these conditions was found to be the same as in the absence of intermolecular exchange, therefore, the intramolecular- and the intermolecular-exchange processes are not correlated.

Base-Initiated Intermolecular Exchange. In view of previous work,²⁻⁶ it was of interest to examine the effect of impurities on the intermolecular process. Thus a sample of 1.0 M $\text{C}_6\text{H}_5\text{PF}_3\text{H}$ and 0.5 M HF in acetonitrile produced an intermolecular-exchange rate of only 100 s^{-1} . This may be compared with the $\text{CH}_3\text{SiF}_4^-$ -HF system³ where 0.005 M HF produced an exchange rate of 2300 s^{-1} . Addition of 0.33 M H_2O to 2.0 M $\text{C}_6\text{H}_5\text{PF}_3\text{H}$ did, initially, produce an intermolecular-exchange rate of 2000 s^{-1} , but this rate decreased to zero within 1 h as $\text{C}_6\text{H}_5\text{P}(\text{O})\text{HF}$ was formed. The hydrolysis product $\text{C}_6\text{H}_5\text{P}(\text{O})\text{HF}$ did not exchange with $\text{C}_6\text{H}_5\text{PF}_3\text{H}$; therefore, neither HF nor H_2O interfered with the study of exchange in $\text{C}_6\text{H}_5\text{PF}_3\text{H}$. An impurity which did, however, affect the exchange process was $\text{C}_6\text{H}_5\text{PF}_4$, as discussed below.

Intermolecular fluorine exchange in $\text{C}_6\text{H}_5\text{PF}_3\text{H}$ was initiated by the addition of small amounts $\sim 10^{-2} \text{ M}$ of triethylamine, pyridine, or other Lewis bases such as 4-methylpyridine, 2,6-dimethylpyridine, and quinoline to 0.3–3 M $\text{C}_6\text{H}_5\text{PF}_3\text{H}$ in solvents such as acetonitrile, nitromethane, benzene, or toluene. All our results suggest that base reacts with $\text{C}_6\text{H}_5\text{PF}_3\text{H}$ to generate the anion $\text{C}_6\text{H}_5\text{PF}_4\text{H}^-$ (eq 4) and that the



rapid intermolecular-exchange process observed in this study corresponds to rapid fluorine exchange between five- and six-coordinate phosphorus species $\text{C}_6\text{H}_5\text{PF}_3\text{H}$ and $\text{C}_6\text{H}_5\text{PF}_4\text{H}^-$, eq 5. Other workers have shown that base and RPF_3H react¹³



according to eq 4, and previous NMR studies have confirmed that fluorine transfer is rapid¹⁴ in the systems PF_5 - PF_6^- and $\text{C}_6\text{H}_5\text{PF}_4$ - $\text{C}_6\text{H}_5\text{PF}_5^-$.

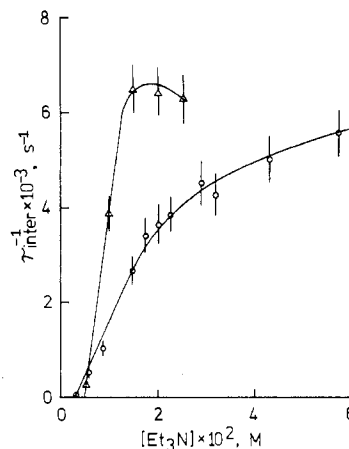


Figure 5. Plot of τ_{inter}^{-1} vs. $[\text{Et}_3\text{N}]$: Δ , $[\text{C}_6\text{H}_5\text{PF}_3\text{H}] = 1 \text{ M}$ in C_6H_6 at 28 °C; \circ , $[\text{C}_6\text{H}_5\text{PF}_3\text{H}] = 1.7 \text{ M}$ in CH_3NO_2 at 34 °C.

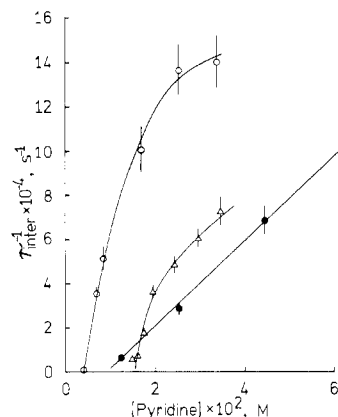


Figure 6. Plot of τ_{inter}^{-1} vs. $[\text{C}_5\text{H}_5\text{N}]$: \circ , $[\text{C}_6\text{H}_5\text{PF}_3\text{H}] = 0.80 \text{ M}$ in C_6H_6 at 28 °C; Δ , $[\text{C}_6\text{H}_5\text{PF}_3\text{H}] = 0.5 \text{ M}$ in C_6H_6 at 22 °C; \bullet , $[\text{C}_6\text{H}_5\text{PF}_3\text{H}] = 3 \text{ M}$ in C_6H_6 at 34 °C.

In support of eq 4, it was found that the amount of $\text{C}_6\text{H}_5\text{PF}_2$ $\sim 10^{-2} \text{ M}$ was approximately equal to the amount of Et_3N or pyridine added to NMR samples of $\text{C}_6\text{H}_5\text{PF}_3\text{H}$. This result was confirmed in a separate reaction by adding $2.5 \times 10^{-4} \text{ mol}$ of pyridine to $2.1 \times 10^{-3} \text{ mol}$ of $\text{C}_6\text{H}_5\text{PF}_3\text{H}$ in 2 mL of benzene. Integration of the ^{31}P NMR spectrum showed a ratio of $\text{C}_6\text{H}_5\text{PF}_2$: $\text{C}_6\text{H}_5\text{PF}_3\text{H}$ of 0.15:1.0. The expected ratio, based on eq 4, is 0.16:1.0. $\text{C}_6\text{H}_5\text{PF}_2$ did not, however, take part in any exchange process which was rapid on the NMR time scale. It was also found that the base-initiated intermolecular-exchange rate required several minutes to reach an equilibrium value, as shown in Figure 4. Such an effect could be observed at low pyridine concentration at 22 °C with an FT NMR spectrometer, but the time interval was shorter at higher base concentration and higher temperature and was difficult to observe with a CW NMR spectrometer. Figure 4 is consistent with the slow production of a reactive species, i.e., $\text{C}_6\text{H}_5\text{PF}_4\text{H}^-$ which then undergoes rapid fluorine exchange. NMR spectra were always recorded after equilibrium was established.

The effect of adding triethylamine to $\text{C}_6\text{H}_5\text{PF}_3\text{H}$ is shown in Figure 2, and a plot of triethylamine and pyridine concentration vs. the intermolecular-exchange rate is shown in Figures 5 and 6. The lines in Figures 5 and 6 do not pass through the origin, instead, a small amount of base must be added before exchange occurs, and, furthermore, the amount of base that is required varies from one sample of $\text{C}_6\text{H}_5\text{PF}_3\text{H}$ to another. Samples of $\text{C}_6\text{H}_5\text{PF}_3\text{H}$ that required larger quantities of base also showed traces of precipitate. The quantity of precipitate did not appear to vary with the quantity of base but rather increased as the concentration of $\text{C}_6\text{H}_5\text{PF}_3\text{H}$ was increased. These observations point to an impurity in

(13) G. I. Drozd, S. Z. Ivin, V. V. Sheluchenko, B. I. Tetel'baum, G. M. Luganskii, and A. D. Varshavskii, *Zh. Obshch. Khim.*, **37**, 1343 (1967); *Chem. Abstr.*, **67**, 108707 (1967); A. H. Cowley, P. J. Wisian, and M. Sanchez, *Inorg. Chem.*, **16**, 1451 (1977).

(14) S. Brownstein and J. Bornais, *Can. J. Chem.*, **46**, 225 (1968); R. Appel, I. Ruppert, and F. Knoll, *Chem. Ber.*, **105**, 2492 (1972).

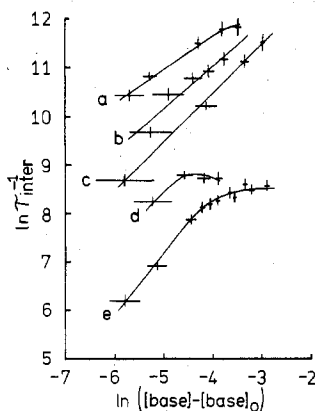


Figure 7. $\ln\text{-}\ln$ plot of data from Figures 5 and 6 using corrected Et_3N and pyridine concentrations: a, pyridine, $[\text{C}_6\text{H}_5\text{PF}_3\text{H}] = 0.80$ M in C_6H_6 at 28°C ; b, pyridine, $[\text{C}_6\text{H}_5\text{PF}_3\text{H}] = 0.5$ M in C_6H_6 at 22°C ; c, pyridine, $[\text{C}_6\text{H}_5\text{PF}_3\text{H}] = 3$ M in C_6H_6 at 34°C ; d, Et_3N , $[\text{C}_6\text{H}_5\text{PF}_3\text{H}] = 1$ M in C_6H_6 at 28°C ; e, Et_3N , $[\text{C}_6\text{H}_5\text{PF}_3\text{H}] = 1.7$ M in CH_3NO_2 at 34°C .

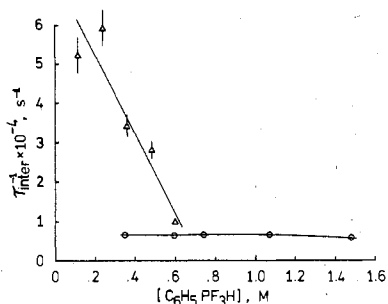


Figure 8. Plot of τ_{inter}^{-1} vs. $[\text{C}_6\text{H}_5\text{PF}_3\text{H}]$: Δ , $[\text{C}_5\text{H}_5\text{N}] = 0.02$ M in C_6H_6 at 22°C with 3 mol % $\text{C}_6\text{H}_5\text{PF}_4$ impurity; \circ , $[\text{Et}_3\text{N}] = 0.025$ M in CH_3NO_2 at 28°C with 0.2 mol % $\text{C}_6\text{H}_5\text{PF}_4$ impurity.

$\text{C}_6\text{H}_5\text{PF}_3\text{H}$ samples which is removing base from NMR samples. By means of NMR and mass spectral analysis and by comparison with an authentic sample, a precipitate was identified as the pyridine adduct of $\text{C}_6\text{H}_5\text{PF}_4$. The impurity $\text{C}_6\text{H}_5\text{PF}_4$ is a decomposition product of $\text{C}_6\text{H}_5\text{PF}_2$, and samples of $\text{C}_6\text{H}_5\text{PF}_3\text{H}$ (prepared from $\text{C}_6\text{H}_5\text{PF}_2$ and HF) were invariably contaminated by 0.2–3 mol % $\text{C}_6\text{H}_5\text{PF}_4$.

If the base concentration is corrected for base that is complexed with $\text{C}_6\text{H}_5\text{PF}_4$, then a log-log plot of exchange rate vs. corrected base concentration should give the order in base. Such a plot is shown in Figure 7. The average slope of the straight line portions of these plots is 1.07 ± 0.21 . Thus, within experimental error, the exchange rate is first order in base, as required by our mechanism which assumes that base produces an equivalent amount of $\text{C}_6\text{H}_5\text{PF}_4\text{H}^-$. The reason for the large error bars in Figure 7 is that the corrected base concentrations involve differences between similar numbers, both of which have uncertainties of 5–10%.

Figures 5–7 also show that the rate of fluorine exchange decreases at higher triethylamine and pyridine concentration;

Table I. Solvents and Intermolecular Fluorine Exchange^a

solvent	$\tau_{\text{inter}}^{-1}, \text{s}^{-1}$	solvent	$\tau_{\text{inter}}^{-1}, \text{s}^{-1}$
acetonitrile	1100	benzene	6400
nitromethane	1680	toluene	8000

^a ^{31}P $\{^1\text{H}\}$ NMR spectra were recorded at 28°C with $[\text{Et}_3\text{N}] = 0.015$ M and $[\text{C}_6\text{H}_5\text{PF}_3\text{H}] = 1$ M.

however, this effect was not investigated further.

Initially, rate studies as a function of $\text{C}_6\text{H}_5\text{PF}_3\text{H}$ concentration were puzzling because they showed a decrease in rate with increasing $\text{C}_6\text{H}_5\text{PF}_3\text{H}$ concentration, as seen in Figure 8; however, this result may be attributed to $\text{C}_6\text{H}_5\text{PF}_4$ impurity. If the line in Figure 8, which corresponds to a sample of $\text{C}_6\text{H}_5\text{PF}_3\text{H}$ containing 0.02 M pyridine and 3 mol % $\text{C}_6\text{H}_5\text{PF}_4$ impurity, is extrapolated to zero rate, then a simple calculation shows that 0.021 M $\text{C}_6\text{H}_5\text{PF}_4$ must be present. In other words, the rate of intermolecular exchange is zero when all pyridine is complexed by $\text{C}_6\text{H}_5\text{PF}_4$ impurity.¹⁵

By choosing a $\text{C}_6\text{H}_5\text{PF}_3\text{H}$ sample which contained as little as 0.2 mol % $\text{C}_6\text{H}_5\text{PF}_4$ impurity, we have shown the exchange rate to be independent of $\text{C}_6\text{H}_5\text{PF}_3\text{H}$ concentration, as seen in Figure 8. Therefore $a = 1$ in eq 3 and the exchange process is first order in $\text{C}_6\text{H}_5\text{PF}_3\text{H}$, as required by the mechanism of eq 5.

The effect of solvent was briefly studied and the results are summarized in Table I. Donor solvents such as acetonitrile or nitromethane suppress the rate of exchange, as compared to solvents such as benzene or toluene. Presumably, any solvent coordination to $\text{C}_6\text{H}_5\text{PF}_3\text{H}$ prevents formation of the fluorine-bridged intermediate of eq 5.

The Arrhenius plot for intermolecular exchange is shown in Figure 3 and $\Delta G^\ddagger_{298} = 7 \pm 2$ kcal/mol and $E_a = 11.5 \pm 0.2$ kcal/mol. The plot is reasonably linear, with slight curvature at lower temperature. Both the intermolecular and the intramolecular rates decrease as the temperature is lowered, and the effect of the intramolecular process is taken into account by the method described in a previous section.

Finally, it has been assumed so far that exchange does not involve the P–H bond in $\text{C}_6\text{H}_5\text{PF}_3\text{H}$. This aspect was readily confirmed by observing the ^{31}P NMR spectrum, without proton decoupling, of a sample of $\text{C}_6\text{H}_5\text{PF}_3\text{H}$ undergoing rapid pyridine-initiated intermolecular fluorine exchange which clearly showed retention of P–H coupling during the rapid fluorine-exchange process. This result also eliminates an alternative pathway of fluorine exchange in which the fluorine ligand is lost as HF.

Acknowledgment. This research was supported by an operating grant from the National Research Council of Canada.

Registry No. $\text{C}_6\text{H}_5\text{PF}_3\text{H}$, 1526-33-6; $\text{C}_6\text{H}_5\text{PF}_2$, 657-97-6; HF, 7664-39-3.

(15) In the $\text{CH}_3\text{SiF}_4\text{-HF}$ system,³ it was also found that fluorine exchange decreased with increasing CH_3SiF_4 concentration. The possibility that an impurity in $\text{Pr}_4\text{N}^+\text{CH}_3\text{SiF}_4^-$ was consuming HF and thereby decreasing the exchange rate cannot be discounted at this time.

(16) W. E. Deming, "Statistical Adjustment of Data", Wiley, New York, 1943.